

The Effect of Cold Deformation on Annealing Behavior of AA3xxx Alloys

Payman Babaghori¹, Warren J. Poole¹, Mary A. Wells² and Nick C. Parson³

¹ Department of Materials Engineering, the University of British Columbia, 309-6350 Stores Road,
Vancouver, V6T 1Z4, Canada

² Department of Mechanical and Mechatronics Engineering, University of Waterloo, 200 University
Avenue West, Waterloo, N2L 3G1, Canada

³ Rio Tinto Alcan, Arvida Research & Development Centre (ARDC), Jonquière, Quebec, Canada

Aluminum alloys particularly AA3xxx alloys are commonly used for heat exchangers due to their good combination of physical and mechanical properties. Post extrusion cold deformation followed by annealing with the objective of controlling the final dimensions of the product can have a significant effect on the microstructure of AA3xxx alloys. The deformation can involve a wide range of strains, for example, a few percent strain for micro-multiport tubing and large strains for tube drawing. The small strain behavior is the particular interest of this study. Often the parts are annealed either as a separate processing step or in conjunction with the brazing operation. The present work shows experimental observations on the microstructure resulting from annealing of the material with different levels of pre-strain and homogenization treatments which modify the dispersoid distribution. Preliminary results have identified the critical strain necessary to initiate recrystallization for different dispersoid distributions and the effect of deformation level on the recrystallized grain size.

Keywords: AA3003; Post-extrusion deformation; Critical strain; Dispersoids; Recrystallization

1. Introduction

AA3xxx series aluminum alloys have made significant inroads by replacing copper in heat exchangers because of their low density, good thermal conductivity, satisfactory mechanical properties and good corrosion resistance. These alloys usually experience a complicated thermomechanical history over a number of processing steps including homogenization, extrusion, cold deformation and then annealing. Often a low level of strain (e.g. 1-8%) is applied to the extruded samples for straightening/sizing before the final heat treatment step. Since the middle of the 1990s, the trend with automotive heat exchangers is to replace the mechanical assembly by brazing of aluminum alloys because of cost, safety and recycling issues [1]. Brazing is generally carried out at high temperatures e.g. 600 °C; hence, dramatic coarsening of the microstructure via a highly inhomogeneous recrystallization process can occur. Results from industry suggest that a wide range of microstructures can be observed ranging from coarse multi-crystals to fine grained polycrystalline microstructures. At a general level, it is known that there is a critical strain/stored energy required to initiate recrystallization [2]. Additionally, it is well established that recrystallized grain size depends on level of cold work, the starting microstructure (grain size, solute content, distribution of 2nd phases), annealing temperature and annealing time. Beyond these general considerations, little has been studied about the recrystallization relevant to the processing of AA3xxx alloys.

Constituent particles, Al₆(Fe, Mn) and very fine particles called dispersoids, α-Al(Mn, Fe)Si are the main intermetallic phases after solidification of AA3xxx series. The as-cast state of these alloys is supersaturated in manganese (Mn) and iron (Fe) at room temperature. During homogenization treatments, dispersoids first nucleate and grow but for longer times, the long range diffusion of Mn to the constituent particles causes the dispersoids to dissolve.

In the present work, the effect of small pre-strains on the microstructure evolution after a brazing simulation has been studied. The study was conducted on the commercially important AA3003

aluminum alloy which is the alloy of choice for use in heat exchanger and cooling system applications.

2. Methodology

2.1 Materials

Two extreme cases in terms of the dispersoid distribution have been examined. Samples of AA3003 were homogenized before extrusion at 600 °C for 1 and 24 hour i.e. one sample with a large density of dispersoids and one with a very low density of dispersoids. Homogenization heat treatment was performed with a heating rate of 150 °C/h, and a heating rate of 50 °C/h for the last hour to the homogenization soak temperature. Table 1 shows the chemical composition of AA3003 alloy. Extrusion was conducted at 480 °C with an exit speed of 100 m/min (billet size: 101 mm × 200 mm, extrusion ratio: 210). Fig. 1 shows the constituent and etch pits caused by dispersoids in the microstructure of the extruded samples (transverse direction: TD).

Table 1. Chemical composition of 3003 aluminum alloy (wt%).

Alloy	Mn	Fe	Si	Al
AA3003	1.25	0.50	0.10	Bal.

2.2 Experimental Procedure

Extruded AA3003 samples with different homogenization practices (i.e. 1 and 24h at 600 °C) were deformed in tension. Two approaches were employed: (a) normal tensile specimen to get specific strains of 1, 2 and 5% and (b) tapered sample to provide a continuous range of strains (Fig. 2a). Tests were conducted with a 5 kN load cell, at a nominal strain rate of $2 \times 10^{-3} \text{ s}^{-1}$. DaVis as an image correlation software and a high speed camera were used to measure the strain along the tapered sample. Afterwards, the cold deformed samples were annealed using the Carbolite™ (HRF) recirculating air furnace. The simulation of brazing was conducted using a 20-minute heat up followed by holding for 2 minutes at 600 °C shown in Fig 2b. The thermal history was obtained by attaching a K-type thermocouple directly to the sample. Thermocouple data was recorded using instruNet™ software and an instruNet Model 100 DAQ.

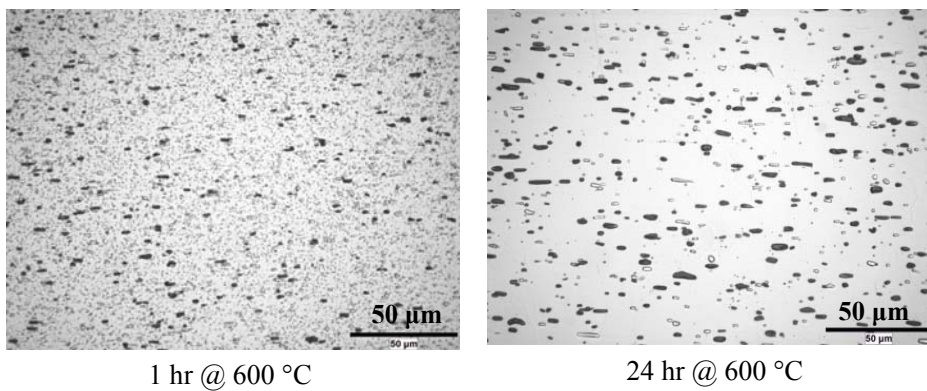


Fig. 1. Constituent and dispersoids distribution in extruded AA3003.

2.3 Characterization of Microstructure and Deformation Behavior

Samples were cold mounted and then metallographically prepared using an automatic grinding and polishing system. Etching of the polished samples was done using a mixture of distilled water and hydrofluoric acid (0.5% volumetric HF) with the intention of revealing intermetallic phases.

A Nikon EPITHOT 300 series optical microscope was used to observe the constituent particles and dispersoids. To study texture and grain orientation, a Hitachi scanning electron microscope,

model S570, operating at 20 KeV was used for electron back scatter diffraction (EBSD) scans. The HKL Channel 5 suite of programs was used to acquire and process the diffraction data. EBSD mapping of the grain structures was carried out at a step size of 1.3 μm . The indexing quality ranges from a minimum of 85% up to as high as 96%. To clean up the map, noise reduction was carried out based on number of the neighbouring pixels.

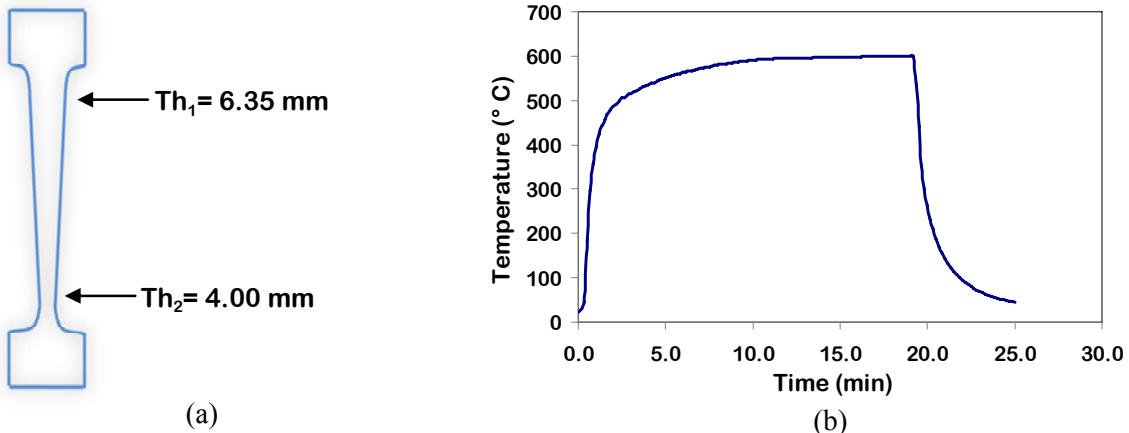


Fig.2. (a) Tapered sample and (b) brazing heat treatment profile obtained from experiment.

3. Results and Discussion

3.1 Characterization of Starting Material

The constituent particles and dispersoids have a significantly different size distribution after heat treatment i.e. constituent particles have a size of 1-5 μm [3] and the dispersoid size is 50-200 nm [4]. For the extruded samples homogenized at 600 $^{\circ}\text{C}$ for 24 hr, almost no evidence of dispersoids were observed. Further, as shown in Fig. 2, the constituent particles are aligned elongated in the extrusion direction. The constituent particles are smaller in the samples homogenized for 1 hour at 600 $^{\circ}\text{C}$ (Fig. 2). The grain structure for the starting materials was also characterized by EBSD as shown in Fig. 3. Pole figures of the two conditions show a relatively strong cubic texture which is a common texture for a recrystallized microstructure [5]. The inhomogeneous distribution of grains as can be seen in EBSD maps of specimens homogenized for 1 hour may be related to the spatial distribution of dispersoids.

Although samples have very different microstructures, the stress-strain response and work hardening rate are only slightly different as shown in Fig. 4. However, this small difference is measurable and, presumably, the differences are associated with the second phase effect. The Kocks-Mecking plot shown in Fig. 4b shows evidence of stage IV, i.e. a near constant work hardening rate at large flow stresses. As such, the Kocks-Mecking model modified by Tomé to include stage IV was fit to the experimental data as shown in Fig. 5, i.e. Tomé et al. [6] have modified the Kocks-Mecking model to include stage IV as follows:

$$\sigma = (\sigma_v + \theta_{IV} \varepsilon^p) \left\{ 1 - \exp \left(-\frac{\theta_0}{\sigma_v} \varepsilon^p \right) \right\} \quad (1)$$

where σ_v is the scaling stress and results from an extrapolation of the work hardening in stage III to zero work hardening rate, θ_{IV} is the rate of work hardening for stage IV (the breakdown the linearity between the work hardening rate and flow stress in stage III), ε^p is plastic strain and θ_0 is the initial work hardening rate. A very good fit to the experimental data was obtained with the values for fit parameters shown in Table 2.

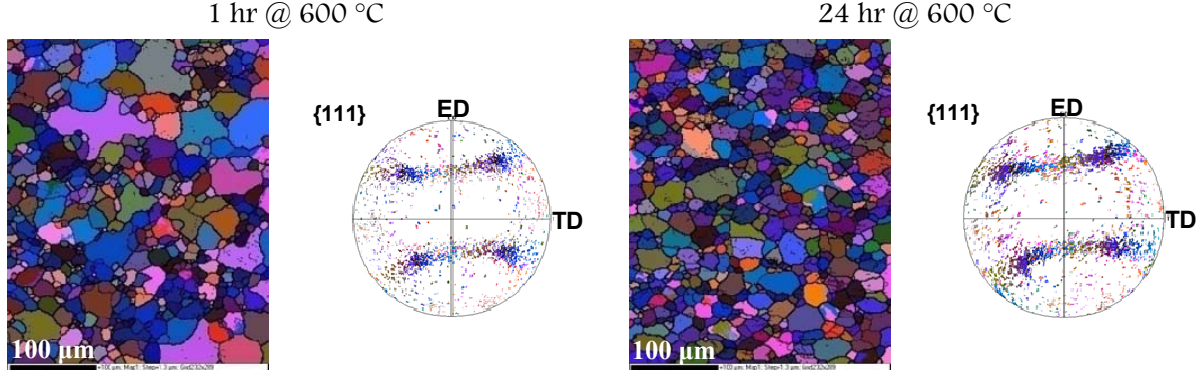


Fig. 3. EBSD maps and pole figures of extruded AA3003 homogenized at 600 °C.

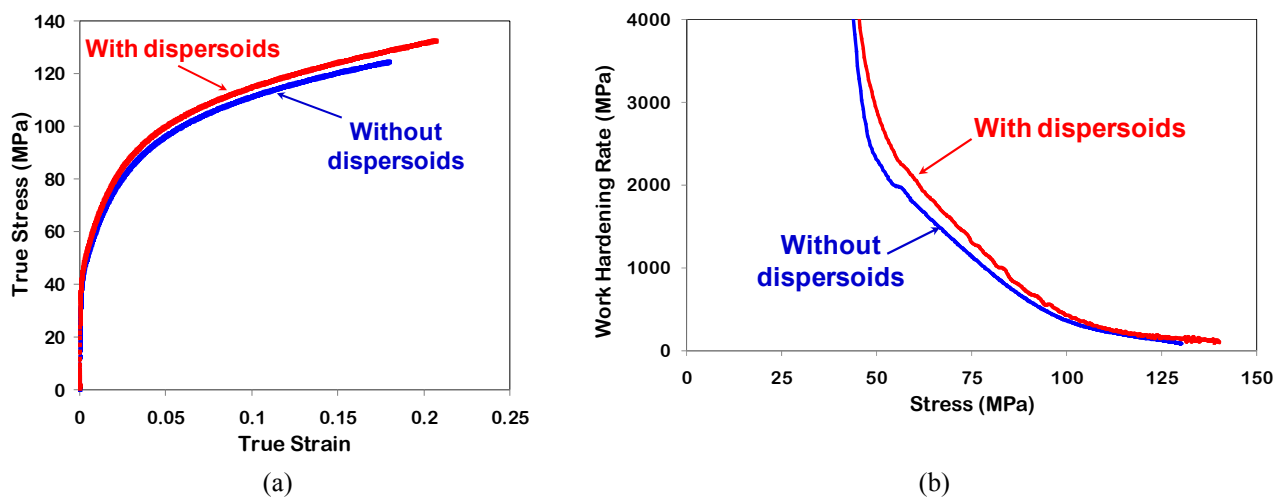


Fig. 4. (a) True stress-true strain curve and (b) work hardening rate-true stress curve.

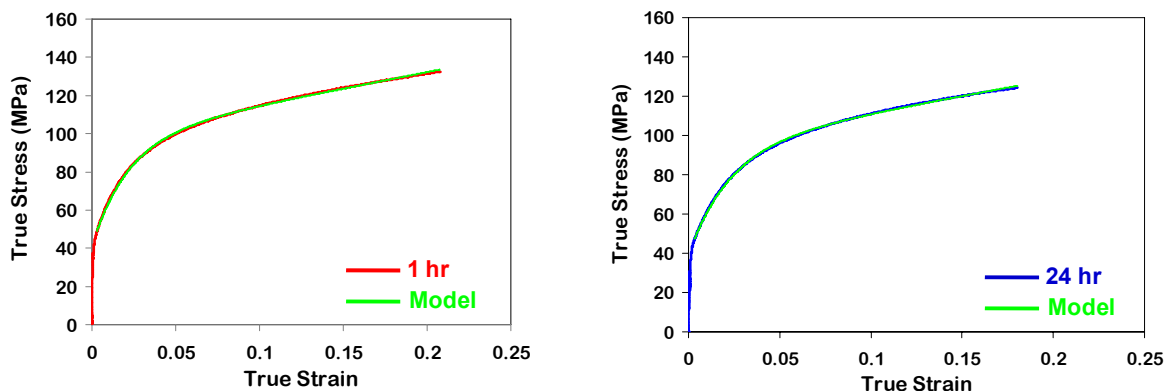


Fig. 5. The Kocks-Mecking model modified by Tomé fitted to the experimental data.

Table 2. Parameters used in the Kocks-Mecking model modified by Tomé.

Fitting Parameters	σ_v (MPa)	θ_0 (MPa)	θ_{IV} (MPa)
1 hr	49	2400	173
24 hr	47	2200	174

3.2 Characterization of Annealed Samples

The distribution and size of the second phase particles (dispersoids and constituent particles) remains the same after the brazing simulation. On the other hand, the grain structure was strongly dependent on the level of cold work as shown in the EBSD maps in Fig. 6. At one extreme, very large

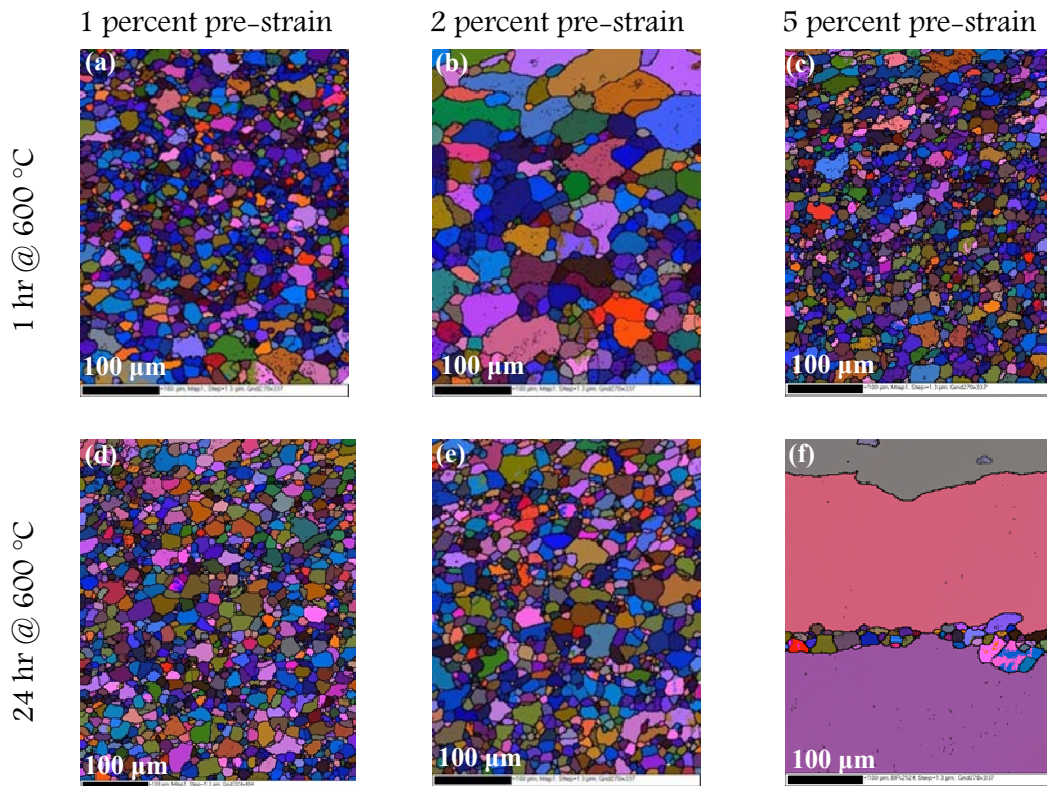


Fig. 6. EBSD maps of pre-strained extruded AA3003 samples after brazing simulation.

grains were observed in the brazed samples with 5% pre-strain which had been homogenized for 24 hr at 600° C prior to extrusion (Fig. 6f). One can speculate that it is related to the critical plastic strain which leads to a small number of recrystallization nuclei. The effect of dispersoids on the recrystallization of the sample can be readily observed by comparing the maps of samples with different homogenization holding time but the same pre-strain, i.e Figure 6c and 6f.

However, in many cases, it is hard to determine whether recrystallization has occurred or not with these low levels of cold work. In order to investigate this further and to determine the critical plastic strain to recrystallization, tapered sample were used. With these samples, there is the possibility to produce one sample with a range of strains along the specimen which can also be characterized using a high speed camera and image correlation software. The strain-position curve shown in Fig. 7a is obtained using DaVis image correlation software. The strain range of 1.5%-7.0% was obtained using tapered samples. Fig. 7b shows the grain size evolution along the tapered sample due to different plastic strains. As expected, three regions exist in the microstructure: (a) unrecrystallized material, (b) recrystallized material with very large grains due to critical plastic strain and (c) recrystallized material with relatively smaller grains as the pre-strain was higher than the critical plastic value.

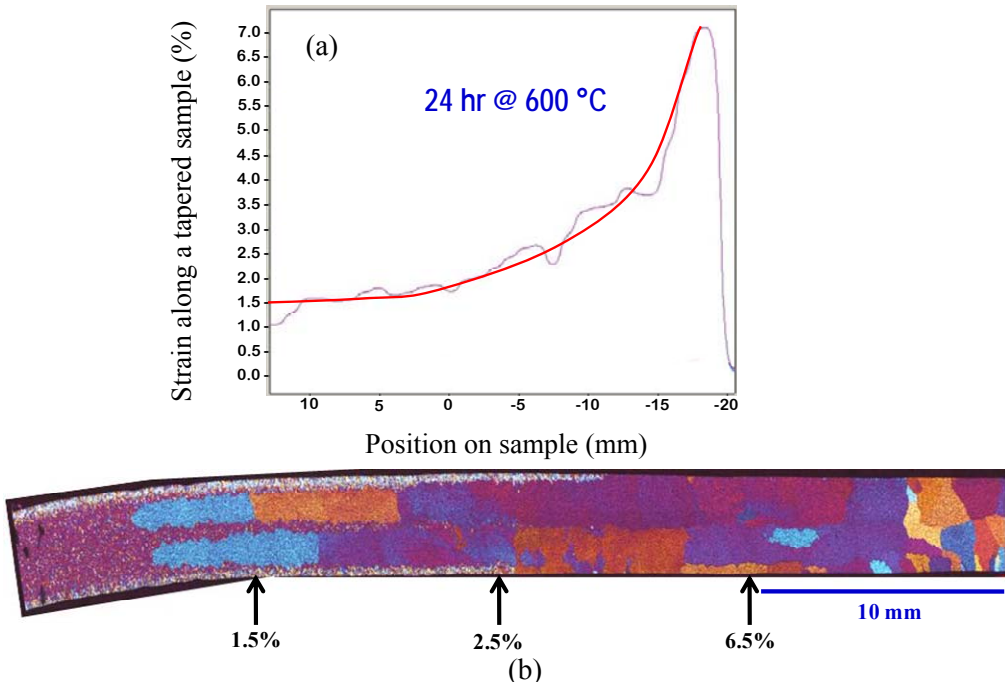


Fig 7. (a) Strain at different sections of a tapered sample obtained from DaVis software, and (b) microstructure along the tapered sample with different plastic strains.

4. Conclusions

- Samples with different homogenization treatments showed small differences in the stress-strain response and work hardening behavior. However, this small difference was measurable and is presumably related to the effect of dispersoids.
- The critical strains necessary to initiate recrystallization was affected by the different dispersoid distributions.
- There is a significant interaction between recrystallization and the second phase particles.
- Recrystallized grain size depends on the level of deformation, i.e. very large grains can be produced at low levels of cold work.

Acknowledgements

The authors would like to gratefully acknowledge the financial support of NSERC (Canada) and Rio Tinto Alcan (RTA). In addition, special thanks are owed to RTA Arvida Research and Development Centre where the alloys were cast and the extrusion trials were conducted.

References

- [1] Y. J. Li, A. Johansen, S. Benum, C. J. Simensen, A. L. Dons, A. Hakonen, L. Arnberg, Aluminium 80 (2004) 578-583.
- [2] J. C. Lashley, M. G. Stout, R. A. Pereyra, M. S. Blau, J. D. Embury, Scripta Mater. 44 (2001) 2815-2820.
- [3] Y. J. Li, L. Arnberg, Mater. Sci. and Eng. A 347 (2003) 130-135.
- [4] Y. J. Li, L. Arnberg, Acta Mater. 51 (2003) 3415-3428.
- [5] F. J. Humphreys, M. Hatherly, Recrystallization and related annealing phenomena, Pergamon, Oxford, UK, 2004.
- [6] C. N. Tome, G. R. Canova, U. F. Kocks, N. Christodoulou, J. J. Jonas, Acta Metall. 32 (1984) 1637-1653.